HHS Public Access

Author manuscript

J Toxicol Environ Health A. Author manuscript; available in PMC 2023 November 18.

Published in final edited form as:

J Toxicol Environ Health A. 2023 August 18; 86(16): 575–596. doi:10.1080/15287394.2023.2226198.

Inhalation of polycarbonate emissions generated during 3D printing processes affects neuroendocrine function in male rats

Kristine Krajnak[a], **Mariana Farcas**[b], **Walter McKinney**[a], **Stacey Waugh**[a], **Kyle Mandler**[b], **Alycia Knepp**[b], **Mark Jackson**[a], **Diana Richardson**[c], **MaryAnne Hammer**[c], **Joanna Matheson**[d], **Treye Thomas**[d], **Yong Qian**[b]

[a]Physical Effects Research Branch, Health Effects Laboratory Division, National Institute for Occupational Safety and Health, Morgantown, WV, USA

[b]Physiology and Pathology Research BranchHealth Effects Laboratory Division, National Institute for Occupational Safety and Health, Morgantown, WV, USA

[c]Histopathology Core, Health Effects Laboratory Division, National Institute for Occupational Safety and Health, Morgantown, WV, USA

[d]Office of Hazard Identification and Reduction, U.S. Consumer Product Safety Commission, Bethesda, MD, USA

Abstract

Three-dimensional (3D) printing of manufactured goods has increased in the last 10 years. The increased use of this technology has resulted in questions regarding the influence of inhaling emissions generated during printing. The goal of this study was to determine if inhalation of particulate and/or toxic chemicals generated during printing with polycarbonate (PC) plastic affected the neuroendocrine system. Male rats were exposed to 3D-printer emissions (592 μg particulate/m^3 air) or filtered air for 4 h/day (d), 4 days/week and total exposures lengths were 1, 4, 8, 15 or 30 days. The effects of these exposures on hormone concentrations, and markers of function and/or injury in the olfactory bulb, hypothalamus and testes were measured after 1, 8 and 30 days exposure. Thirty days of exposure to 3D printer emissions resulted in reductions in thyroid stimulating hormone, follicle stimulating hormone and prolactin. These changes were accompanied by (1) elevation in markers of cell injury; (2) reductions in active mitochondria in the olfactory bulb, diminished gonadotropin releasing hormone cells and fibers as well as less tyrosine hydroxylase immunolabeled fibers in the arcuate nucleus; and (3) decrease in spermatogonium.

CONTACT Kristine Krajnak ksk1@cdc.gov Histopathology Core, Health Effects Laboratory Division, NIOSH, 1000 Fredrick Lane, Morgantown, WV 26505, USA.

Disclosure statement

No potential conflict of interest was reported by the author(s).

Disclaimer

The findings and conclusions in this manuscript are those of the authors and do not necessarily represent the views of the National Institute for Occupational Safety and Health, Centers for Disease Control and Prevention and the U.S. Consumer Safety Product Commission. This work has not been reviewed or approved by and does not necessarily represent the views of the U.S. Consumer Product Safety Commission. Certain commercial equipment, instruments, or materials are identified in this paper to specify the experimental procedure adequately. Such identification is not intended to imply recommendation or endorsement by the Consumer Product Safety Commission, nor is it intended to imply that the materials or equipment identified are necessarily the best available for the purpose.

Polycarbonate plastics may contain bisphenol A, and the effects of exposure to these 3D printer-generated emissions on neuroendocrine function are similar to those noted following exposure to bisphenol A.

Keywords

Inhalation; 3D printing; neuroendocrine; males

Introduction

Over the last 10 years there has been an increasing concern regarding how plastic particles (particles <1 μm in diameter) in the environment may affect the health of humans and wildlife (Burgos-Aceves et al. 2022; GM et al. 2017; Martín et al. 2018; Roberts et al. 2014; Rubio, Marcos, and Hernandez 2020). With the increased use of 3D printers in manufacturing settings and schools, humans are now also exposed to inhalable plastic nanoparticles (plastic particles <100 nm in diameter) generated during the printing process (Chan et al. 2020; Farcas et al. 2019, 2020). Although many investigators determined the influence of environmental exposure to plastic particles on the health of aquatic species (Burgos-Aceves et al. 2022; Dmytriw 2020; Martín et al. 2018; Suhyun et al. 2019), fewer studies examined the influence of inhalation of plastic nanoparticles (NP) and their composite chemicals on human health (Azimi et al. 2016; Dmytriw 2020; Martín et al. 2018; Rubio, Marcos, and Hernandez 2020; Stefaniak et al. 2017). 3-Dimensional printing (3DP) generates both respirable plastic nanoparticles and volatile chemicals (Azimi et al. 2016; Chan et al. 2020; Farcas et al. 2019; MT et al. 2020; Stefaniak et al. 2017; Wu et al. 2020). Because of the increased use of 3DP for production of plastic products in manufacturing settings, schools and homes, and the potential for exposure to high concentrations of aerosolized NP and volatile chemicals, there has been rising concern regarding the effects of inhaling 3DP emissions (Sharma and Chatterjee 2017; Wright and Kelly 2017).

A number of different plastic composites, including acrylonitrile butadiene styrene (ABS), poly-lactic acid (PLA) and polycarbonate (PC) are used in 3DP processes (Azimi et al. 2016; Leso et al. 2021; Stefaniak et al. 2017; Yi et al. 2016). In addition to the potential effects of inhaled plastic particulate, 3DP plastic filaments often contain other potentially toxic chemicals that are aerosolized when the filament is heated (Yi et al. 2016; Stefaniak et al. 2017). One chemical that might be released is bisphenol (BP), and there is evidence that inhalation of BPs exerts adverse health effects (Catenza et al. 2021; Chung et al. 2017). Acrylonitrile and BPs might act as endocrine disrupters by mimicking the effects of endogenous estrogens (Suhyun et al. 2019; Ullah et al. 2018). These chemicals disrupt endocrine systems, including the thyroid- and adrenal-pituitary axes (Suhyun et al. 2019; Ullah et al. 2018). Previously investigators demonstrated adverse respiratory and cardiovascular effects attributed to inhalation of 3DP emissions (Farcas et al. 2019, 2020; Stefaniak et al. 2017) and these findings served to fill knowledge gaps on the potential systemic toxicological effects attributed to exposure to 3DP emissions. The current investigation is postulated to assist in the efforts to establish effective control strategies and

exposure limits for specific materials to prevent adverse health effects attributed to 3DP emission exposure.

The goal of this study was to determine whether exposure to emissions (a mixture of organic gasses and aerosols) resulted in changes in markers of neurotoxicity in the olfactory bulb and in regions of the brain that regulate neuroendocrine processes in Sprague-Dawley (SD) rats. The olfactory bulb was examined because olfactory cues regulate reproduction and feeding behaviors (Persaud 2013; Powers and Winnans 1973; Slotnick and Coppola 2015; Vandenburgh 1973). The olfactory bulb and the circulation may provide pathways for particulate matter (PM) to access to the brain via the circulation or by transport via the olfactory system (Hubbs et al. 2011). Therefore, regions of the brain that receive input from the olfactory system, or have a less effective blood brain barrier (BBB), may be more likely to be exposed to emissions generated by 3D printing. In addition, inhalation of 3DP emissions might disrupt the transmission of olfactory cues to regions of the brain that regulate feeding or reproductive behaviors and interfere with the release of hormones involved in mediating reproduction and metabolic processes in animals (Slotnick and Coppola 2015). 3DP emissions may also contain plastic particulates and release bisphenol A (BPA) during the printing process, or possibly when inhaled 3DP particulate is dissolved in the body, BPA may be released from the particulate. Exposure to BPA might affect health by interfering with the release of gonadal steroids and anterior pituitary hormones that regulate reproductive, developmental and metabolic processes (Abraham and Chakraborty 2019; Chung et al. 2017; Cimmino et al. 2020; Lehmler et al. 2018; Mustieles et al. 2015; Ullah et al. 2018). Based upon previous findings, the aim of this study was to determine whether inhalation of emissions generated by 3DP using PC printing stock (which contains BPA), induces reproductive and metabolic dysfunction by affecting olfactory and/or hypothalamic-pituitary-gonadal/metabolic pathways in SD rats.

Methods

Animals

Male Sprague Dawley rats ([H1a: (SD) CVF, $n = 6$ rats/group ($N = 60$); 6–7 weeks of age, 200–250 g) were obtained from Hilltop Lab Animals, Inc., Scottdale, PA. Males were used in this study because the inhalation model has been characterized in males (Farcas et al. 2020). The responses of females to the exposure will be assessed in future studies. All animals were free of viral pathogens, parasites, *Mycoplasma*, *Heliobacter* and cilia-associated respiratory (CAR) bacillus. Rats were acclimated to the facilities for 1 week after arrival and housed in polycarbonate cages (Lab Products LLC, Aberdeen MD) with Teklad Sani-chip bedding (Envigo, Madison WI) and ventilated with HEPA-filters under controlled temperature and humidity conditions and a 12-hr light/dark cycle. Food (Teklad 7913; Envigo Madison, WI) and tap water were provided *ad libitum*. The animal facilities are specific pathogen-free, environmentally controlled, and accredited by AAALAC International. All procedures were approved by the CDC-NIOSH Morgantown Animal Care and Use Committee and were in compliance with the Public Health Service Policy on Humane Care and Use of Laboratory Animals and the NIH Guide for the Care and Use of Laboratory Animals.

Exposure

After 1 week of acclimation to the facility, animals were exposed to filtered-air (controls) or emissions generated by 3DP as described in (Farcas et al. 2019). Briefly, animals were placed in separate compartments of a whole-body exposure chamber that could hold up to 12 animals. There was no food or water available during the exposure. The cage rack with the animals rested on top of cage support beams which contained 1 cm outside diameter stainless steel tubes with small holes. Each hole was placed in the center of the cage partition so that aerosols would be drawn into the breathing space. Three desktop 3D printers (LulzBot Mini, Fargo Additive Manufacturing Equipment 3D LLC, Fargo, ND) were placed in an airtight chamber. Black polycarbonate filament (Gizmo Dorks LLC, Temple City, CA 3D Printing Polycarbonate Filament – Gizmo Dorks) was fed into each printer and the printers were operated continuously during the 4 hr exposure period. At the beginning of each exposure, animals were placed into the designated chamber (for air or 3DP emission exposure). Emissions from the printing chamber or filtered air were pumped into the whole-body inhalation chamber. At the end of each exposure, animals were placed into their home cages and returned to the colony room.

Emissions generated in the exposure chamber were discharged into the chamber with the animals. Specific parameters used to generate the emissions are presented in Table 1. Exposures were monitored as previously described (Farcas et al. 2020). The mean hydrodynamic particle size and particle concentrations were measured using nanoparticle tracking system analysis (NTA; NanoSight NS300, Malvern Instruments, Worcestershire, UK). The measured particulate emissions inside the exposure chamber averaged 592 $\mu g/m^3$ of particulate for a 4 hr exposure when the mean was calculated over all days of the exposure (Figure 1). A typical size distribution plot (particle count based) of the PC particles inside the exposure chamber during a test run is illustrated in Figure 2a. Particulate was collected every 5 sec and particle size was measured using a fast mobility particle sizer (size range 5.6–560 nm, model 3091 TSI Inc, Shoreview MN) Figure 2b illustrates the particle size distribution was converted to aerodynamic equivalent mass by assuming all particles were spherical and had a density of 1.2 g/cm^3 (the density of polycarbonate). The mean particle electric mobility diameter for every 5 sec sample during four separate 4 hr test runs is depicted in Figure 2c. The mean aerodynamic equivalent diameter measured inside the exposure chamber during the print jobs was 40 nm. The PC particles were also collected on filters and imaged with a scanning electron microscope. Typical physical diameters for PC particulate ranged from 40 nm up to 90 nm (Farcas et al. 2019).

Analysis of volatile organic compounds by GC/MS

The volatile organic components of the 3DP emissions were analyzed by GC/MS from samples collected over a 4 hr collection period (Table 2). The measurement of volatile compounds was conducted using a method published in the NIOSH Analytical Methods Manual (2018; 3900: Volatile organic compounds (VOC), C1 to C10 canister method; are found at https://www.cdc.gov/niosh/nmam/default.html). The levels of measured compounds were low, with acetaldehyde, acetone, ethanol, and ethylbenzene levels being the highest among the detected compounds. Table 2 presents the levels (ppb) of VOC measured in this study and Occupational Safety and Health Administrations (OSHAs) permissible

exposure limits (PELs). Although different methods are used for measurement, none of the compounds measured in this experiment were above the PELs.

Bisphenol A and bisphenol A diglycidyl ether were also assessed in the 3DP-generated emissions. Sampling for these substances occurred under the same conditions used to generate the animal exposures, except the animals were not in the chamber. The total concentration of particulate in each sample was approximately 600 μg/m^3. The emissions were collected onto glass fiber filters (SKC lot #21600–7E5–274; n = 6 samples) and filters analyzed by BVNA labs (Novi, MI). Once received by BVNA, the filters were placed in separate glass test tubes and each sample cassette was wiped with a glass fiber filter wetted with 100% ethanol. Sample filters and wipes were extracted in 3 ml acetonitrile and then placed on a mechanical flatbed shaker for 30 min. An aliquot (18 μl) was transferred to individual auto-sampler vials for analysis by HPLC (Thermo Fisher Vanquish UHPLC with a Zorbax ODS C18, 5 μM 250 mm × 4.4 mm internal diameter). Samples were analyzed using a wavelength of 230 nm and read time of 22 min/sample. The average level of bisphenol in the samples was 5.3 ± 0.18 μg/m^3. Using a mass particle distribution model to determine particle deposition in the nose, trachea, alveola and lung (where the tidal vol is 1.7 ml, the breathing rate is 120 breaths/min and the exposure time is 240 min), the estimated cumulative deposition of bisphenol A in the entire respiratory tract was 36 ng on day 1, 536 ng on day 15 and 1.072 μg on day 30. Bisphenol A diglycidyl ether was not detectable in any of the samples.

Tissue collection

Animals were exposed to air or 3DP emissions for 4 hr/day. Animals in the 1 day exposure group were exposed for 1 day. Animals in all other groups were exposed 4 day/week until the required number of days of exposure (4, 8, 15 or 30 days) was reached. Body weights were collected the day following the last exposure. Groups of animals (6 air control and 6 3DP-exposed) were euthanized by injection of pentobarbital euthanasia solution (100 mg/kg i.p.) and exsanguinated 24 hr after 1, 4, 8, 15 or 30 days of exposure. Animals were exsanguinated by collecting blood from the descending aorta into EDTA treated tubes. The blood was kept on a shaker for approximately 1 hr and centrifuged at 10,500 g for 15 min at 4°C. Plasma was pipetted into 200 μl aliquots and frozen at − 80°C until assayed. The brain was dissected and cut into right and left hemispheres. The olfactory bulb and hypothalamus were dissected from the right hemisphere of the brain and frozen at − 80°C until used for PCR. The left hemisphere was placed in Tissue-Tek OCT compound (Fisher Scientific) in a cryomold and frozen at − 80°C until sectioned and processed for immunohistochemistry and histology.

Tissue preparation: Histology

The left hemisphere of the brain was sectioned (20 μm) using a cryostat set at − 20°C. Five slides were collected from the olfactory bulb and hypothalamus. The first section was put on slide 1, the second section on slide 2 and continuing through to the 5th section on slide 5. Using this procedure there was 100 μm between consecutive sections on each slide. There were 5–6 sections/slide from the olfactory bulb and 3–4 sections/slide from the hypothalamus of each animal. Using this method, each slide contains a section through

the rostral to caudal portions of a brain region. For histological or immunohistochemical analyses, one slide from each animal and each region was processed.

The right testis was also dissected from each animal and placed in 10% buffered formalin. Each testis was paraffin embedded and sections (10 μm) were cut on a microtome. Five slides were collected from each animal, with each slide having one or two tissue sections. One set of sections was stained with Harris hematoxylin and eosin for histological analyses. The others were stored at room temperature until used for immunohistochemistry.

Histology and Immunohistochemistry

Immunohistochemistry was performed using a previously described protocol with slight modifications (Johnson et al. 2016; Krajnak et al. 2013). Briefly, slides were fixed in 4% paraformaldehyde in 0.1 M phosphate buffered saline (PBS) for 5 min, rinsed 3 × 5 min in PBS and incubated in primary antibody diluted in 0.1 M PBS plus 0.3% Triton-x 100 (Tx) and 10% normal serum overnight at 4°C. Immunohistochemistry and histological stains were used on sections of the olfactory bulb to determine levels of glial derived neurotrophic factor (GDNF), tyrosine hydroxylase (TH), Mitotracker orange and myelin basic protein (MB).; In the hypothalamus staining for Mitotracker orange, Fluoro-Jade, TH and gonadotropin releasing hormone (GnRH) was performed. Staining for luteinizing hormone receptor (LHr) and follicle stimulating hormone receptor (FSHr) was performed in the testes. A list of primary antibodies, the manufacturer, and the dilutions used for each antibody is presented in Table 3. The following day the slides were rinsed, and sections incubated with the secondary antibody (either Cy3 or fluorescein labeled antibodies; Jackson Immunolabs) diluted 1:500 in 0.1 M PBS-Tx at RT for 1 hr. Sections were then rinsed, air dried and cover-slipped using Prolong Gold with 4’6-diamindino −2-phenylindole (DAPI, Invitrogen, Waltham, MA).

Another set of sections was labeled using Fluoro-Jade C (Sigma Chemicals, St Louis, MO) which identifies damaged neurons. A stock solution of Fluoro-Jade (3.0% in dimethyl sulfoxide (DMSO)) was aliquoted and frozen at − 20°C until use. For staining, sections were fixed as described above, incubated in a 0.06% potassium permanganate solution in 0.1 M PBS for 10 min, rinsed and then incubated in the Fluoro-Jade solution (0.003% in 0.1 M acetic acid) for 1 hr, in the dark, at room temperature. Sections were then rinsed in water and cover slipped as described above. Staining in the periventricular/arcuate nuclei was measured because the neurons that regulate pituitary function are primarily located in these regions. The % area labeled was measured using Image J (National Institutes of Health (NIH), Bethesda MD). Labeling was measured in 3–5 sections per animal and the average labeled area was calculated and employed for analyses. Gonadotropin releasing hormone (GnRH) and TH neurons were also counted in these nuclei.

To label mitochondria Mitotracker Orange CMTMRos (Invitrogen, Waltham, MA) was used. This specific Mitotracker stain enters the cell and is oxidized to its fluorescent form which is then sequestered in active mitochondria. To perform staining, stock solution supplied by the manufacturer was thawed and diluted to 500 nM using 0.1 M PBS. Slides were incubated in diluted Mitotracker for 30 min at 37°C, rinsed 3 × 5 min in PBS, incubated in 4% paraformaldehyde in 0.1 M PBS for 10 min, dried, cover-slipped using Prolong

Gold with DAPI, and stored in a light tight container at 4°C. Mitotracker staining was quantified by visualizing the sections using fluorescent microscopy at a wavelength of 554/576 nm (excitation/emission). Both the % area labeled, and the intensity of the labeling were measured using Image J (NIH). Labeling was measured in 3–5 sections per animal and the average labeled area and intensity were calculated and employed for analyses.

For paraffin embedded sections of the testes, slides were first heated at 60°C for 20 min and then incubated in 3 rinses of xylene (20 min each at room temperature) to remove the paraffin. Sections were then dehydrated using decreasing concentrations of ethanol (100–75%) and rehydrated in water followed by 0.1 M PBS. One slide was stained with Harris hematoxylin and eosin (H&E) stain, and the number of Sertoli cells, Leydig cells and spermatogonium were counted in four photomicrographs/animal. The number of mature sperm was determined by measuring the density of the sperm tails in the seminiferous tubules. Other slides were utilized for immunohistochemistry, which was performed as described above.

Microscopy

Fluorescent-labeled slides were examined using an Olympus microscope; photomicrographs were taken at a magnification of 20× using DP73 camera and CellSense version 510 (B&B Microscopes, Pittsburgh, PA). Densitometry was performed on photomicrographs using ImageJ. To perform densitometry, a threshold was set to identify regions that were immuno-stained. The area to be quantified was outlined and the total area of the outlined structure was measured along the with area of the immunolabeled cells that were at or above the set threshold. Depending on the region, 3–5 sections were analyzed. The average immune-stained area was calculated and used for analyses.

A stereological method was used to quantify structures in the testes, a stereographic procedure utilizing a grid was utilized to count the number of Sertoli cells, spermatocytes at different stages of development and Leydig cells. The grid used for counting was a 12.5 mm square consisting of 100 smaller squares (Baker et al. 2007). The number of cells or structures within each box of the grid was counted, the number of cells or structures that intersected with either a vertical or horizontal line of the grid was counted. Three to five sections were analyzed from each animal. An average number of cells/section was calculated and employed for analyses.

Enzyme linked immunosorbent assays (ELISAs)

ELISAs for estradiol, prolactin, thyroid stimulating hormone (TSH) and follicle stimulating hormone (FSH) were performed using plasma samples collected from animals after 1, 4, 8, 15 or 30 days of exposure. ELISAs for estrogen and prolactin were purchased from Calbiotech (El Cajon, CA), and for TSH and FSH from E-Lab Sciences (Houston, TX). All assays were run according to the manufacturer's protocols. Measurement of these hormones were selected based upon previous studies that demonstrated that these hormones might be altered by endocrine disrupters such as bisphenol A (Abraham and Chakraborty 2019; Chung et al. 2017; Cimmino et al. 2020; Lehmler et al. 2018; Mustieles et al. 2015; Ullah et al. 2018). The measured coefficients of variation for each assay were as follows: estrogen

11.5%; FSH 3.6%; prolactin 2.33% and TSH 6.46%, and the limits of detectability were 0. To control for potential variability in the plate or the plate reader, one sample and one standard were pipetted on the plate and read before and after the experimental samples. The variation in these replicates was less than the coefficient of variation for each assay.

Quantitative reverse transcriptase polymerase chain reaction (qRT-PCR)

qRT-PCR was performed to determine if exposure to 3DP emissions resulted in changes in transcript levels in the olfactory bulb and hypothalamus as described in Krajnak et al. (2013). RNA was isolated from the tissue using RNAeasy lipid Miniprep kits (cat # 74804; Qiagen, Valencia, CA), and first strand cDNA was synthesized from 1 μg total RNA using a Reverse Transcription System (Invitrogen; Carlsbad, CA). Melt curves were run for each transcript using each tissue. Samples that did not exhibit a single defined melt peak in the 80°C range were not included in the dataset. To determine if the treatment resulted in a change in transcript levels, fold changes from same day controls were calculated. This was done by calculating the mean response for the control group and then subtracting the individual CT values for each sample from the average of the controls. Transcripts were measured in the olfactory bulb (Table 4) and hypothalamus (Table 5) and included immediate early genes, glial cell, oxidative stress and inflammatory markers and markers of proteins involved in neurotransmission.

Data analyses

Fold changes in transcript levels and stereological data were analyzed using 2 (control vs exposed) × 5 (time points) analyses of variance (ANOVAs). ELISA data and immune-histochemical data were analyzed using a 2 (control vs exposed) × 2–3 (time points) ANOVAs. Pairwise comparisons between groups were performed using t-tests. Comparisons with $p < 0.05$ were considered significantly different.

Results

Body Weight

Figure 3 presents the influence of exposure to 3DP emissions on body weights. Body weights were collected the day following their last exposure. Animals in both the air control and 3DP emission groups displayed growth, as measured by changes in body weight over the course of the experiment. However, after 4 days of exposure, animals exposed to 3DP displayed lower body weights than air-control animals and this reduction in body weight was significant after 15 or 30 days of exposure.

Circulating hormone concentrations

Plasma from the animals in this experiment was used by a number of different investigators. Because there was not sufficient sample to measure all hormones at all time points, it was of interest to examine circulating hormone concentrations after 1 and 30 days of exposure. Average circulating TSH concentrations (Figure 4A) were generally lower in animals exposed to 3D printer emissions than levels in air control animals, and after 30 days exposure, this difference was significant. In addition, TSH concentrations in both air- and 3D printer emission-exposed animals were decreased after 30 days than after 1 day

treatment. Average circulating FSH concentrations (Figure 4B) were not measurable in any of the control animals after 1 day exposure (the lower limit of detection was approximately 1.5 ng/ml) but were measurable in 4 out of 6 animals exposed to 3DP emissions. However, even in exposed animals, FSH levels were near the limit of detection. The lower levels of FSH seen on the first day of the experiment may have been due to stress associated with the first day of treatment. The higher levels in 3D printer emission exposed animals may have been due to effects associated with inhalation of the emissions. After 30 day exposure, FSH concentrations in air control animals were concentrations normally detected in adult males, while animals exposed to 3D printer emissions demonstrated significantly diminished circulating concentrations. Average circulating prolactin concentrations declined over the course of the experiment in 3DP emission exposed animals (Figure 4C), with levels significantly reduced than in control animals after 30 day treatment. Average circulating estradiol concentrations did not markedly change at any time point for either exposure group (Figure 4D).

Immunohistochemistry and Histology

To determine if exposure to 3DP emissions resulted in injury to cells or possible changes in cellular function, the area immunostained was measured for glial-derived neurotrophic factor (GDNF), TH, Mitotracker orange and myelin basic protein (MBP) in the olfactory bulb. GDNF did not markedly change with treatment but was lower after 8 day exposure to air and 3DP emissions than after 1 day treatment. After 30 day exposure, GDNF staining increased, but the stained area was still significantly less than it was after 1 day. TH labeling was also measured in the olfactory bulb. The area stained for TH was significantly lower in the olfactory bulbs of 3DP emission-exposed than air-exposed animals after 30 days (Figure 5B). Alterations in mitochondrial function due to exposure to printer emissions was assessed by measuring the area of olfactory bulb sections stained with Mitotracker (Figure 5C). There were no significant changes in Mitotracker staining area following 1day treatment. However, after 8 days of exposure, there was a significant decrease in the stained area in both air and 3DP emission exposed animals. After 30 day treatment, Mitotracker staining in air controls returned to 1day levels. However, Mitotracker staining in 3DP emission exposed olfactory bulbs was still significantly reduced compared to 30 day air controls. Myelin basic protein (MBP) immunostaining in the olfactory bulb was generally diminished in 3DP emission exposed than air control animals at all time points (Figure 5D), and this difference was significant after 1 and 8 day exposure. After 30 day treatment MBP staining in both control and emission exposed olfactory bulbs was comparable to that noted after 1 day.

Staining for indicators of oxidative stress, injury and neuroendocrine function were also examined in the hypothalamus (Figure 6). Mitotracker staining (Figure 6a) increased in the hypothalamus in both exposure groups. Fluoro-Jade staining (Figure 6b) was examined to determine if exposure to 3DP emissions resulted in any neural damage. There were no treatment or time related differences in Fluoro-Jade staining in either the air or 3DP emission exposed animals. Both the area of TH immunopositive staining (Figure 6c) and the mean number of labeled cells/section in the hypothalamus were counted (Figure 6d). Elevation in the region immunostained for TH were observed in the hypothalamus of both treatment groups between 1 and 8 day exposure. After 30 day treatment, the area

stained with TH returned to day 1 levels in both groups of animals. TH cell number in the hypothalamus (Figure 6d) increased in both groups of animals after 8 day exposure. However, after 30d ay treatment, TH cell number declined to day 1 levels in 3DP emission exposed animals. Figure 6e, f illustrate the area and average number of cells/section that were immunostained for GnRH. After 8 and 30 days exposure to air, the area stained with GnRH was greater than day 1 air controls and 3DP emission exposed animals (Figure 6e). GnRH immunolabeled cell number was elevated in both air and 3DP emission exposed animals after 8 day exposure and in air-exposed controls after 30 days (Figure 6f). However, after 30 day treatment, cell number in the 3DP-emission exposed animals returned to day 1 levels and the number of cells was significantly lower than that seen in air-exposed animals.

The area immunolabeled for the luteinizing hormone (LHr; Figure 7a) and follicle stimulating hormone (FSHr; Figure 7b) receptors was also examined in the testes because these receptors may regulate the ability of LH and FSH to induce gamete production and steroidogenesis. Neither exposure condition nor exposure length influenced the area stained for either receptor.

Data collected to determine if exposure to 3DP emissions resulted in changes in testicular morphology is presented in Figure 8. Animals in both treatment groups showed a reduction in the number of Sertoli cells in the testes (Figure 8a–c), however in 3DP emission exposed animals, the reduction was greater at 8 days than it was in air exposed animals. In control animals, the number of Sertoli cells was lower after 30 day treatment than after 1day. The number of Leydig cells decreased between 1 and 8 days exposure, with cell number in 3DP emission-exposed animals diminished than those in air exposed (Figure 8A, 8B,8 D). Spermatogonium number decreased in 3DP emission exposed animals through the exposure periods, with numbers at 30 days significantly lower than day 8 (Figure 8a–e). The density of mature sperm in the testicular lumen of 3DP-emission exposed animals was elevated after 8 day exposure as compared to sperm levels after 1 day and as compared to mature sperm levels in control animals. After 8 day treatment, sperm levels were higher in both treatment groups than levels after 1 day. However, after 30 days of 3DP exposure mature sperm levels returned to levels detected after 1 day.

Transcript expression

Mean ± SEM transcript levels measured in the olfactory bulb are presented in Table 4. There was a significant reduction in *c-Fos* expression after 4 days of exposure and a rise in expression 30 days after exposure to 3DP emissions. The expression of the antioxidant superoxide dismutase (*Sod2*) was not markedly affected by exposure to 3DP emissions, but catalase (*Cat*) was reduced in the olfactory bulb after exposure to 3DP emissions at all timepoints. The expression of the pro-inflammatory factor tumor necrosis factor (*Tnf*)-*α* was significantly increased after 15 days exposure and the expression of the growth factor, glial-derived neurotrophic factor (*Gdnf*) was decreased after 1 day but elevated after 8 days of exposure to 3DP emissions.

In the hypothalamus, transcripts for factors involved in mediating vascular function, cell signaling, reproduction, pain, oxidative stress and glial growth were assessed (Table 5).

There were no significant day- or exposure-induced alterations in transcript expression in the hypothalamus.

Discussion

Plastic particulate and chemicals used in the production of plastics are released into the environment when plastics are heated or placed in a solution. The emissions from these plastics were reported to produce adverse health effects in both aquatic and land species (Burgos-Aceves et al. 2022; Dmytriw 2020; Martín et al. 2018; Rubio, Marcos, and Hernandez 2020; Suhyun et al. 2019). Recently, the use of 3D printers has increased, and there are data demonstrating that 3D printers used in areas that are not properly ventilated might generate and release high concentrations of respirable particulate and volatile vapors that may also affect health (Chan et al. 2020, Yi et al. 2016; Kim et al. 2015; Leso et al. 2021; Vaisanen et al. 2022). The exact characteristics of the exposure, and the physiological and biological effects of the exposure, are dependent upon the concentrations and types of PM and VOC released during the printing process (Farcas et al. 2019; MT et al. 2020). The goal of the current study was to (1) determine what types of emissions were generated when printing with PC stock, and (2) assess the impact of this exposure on reproductive and neuroendocrine function.

Based upon the results of this study, evidence indicates that inhalation of 3DP emissions affects olfactory, neuroendocrine and reproductive function, and that these effects may be due to 3DP generated PM or VOC at various levels of the olfactory and hypothalamic/pituitary/gonadal or thyroid (metabolic) axes. The effects of the exposure on neuroendocrine function are similar to those seen in animals exposed to BPA (Cimmino et al. 2020; Lehmler et al. 2018; Skledar and Masic 2016; Ullah et al. 2018). Bisphenol A concentrations measured in the PM in this study were lower than levels used to induce neuroendocrine effects in other published studies. There are other bisphenols in plastics might exert endocrine disrupting effects (Lehmler et al. 2018; Ullah et al. 2018). However, investigations measuring the various components of emissions generated by 3DP demonstrated that only BPA is measurable in PM generated by 3DP with polycarbonate stock (Stefaniak et al. 2021). In addition, most of the other studies cited used an oral route of exposure (Lehmler et al. 2018; Li et al. 2020; Ma et al. 2019; Mustieles et al. 2015; National Toxicology Program 2021; Rochester 2013; Skledar and Masic 2016; Vasiljevic and Harner 2021).There is one inhalation study that examined the impact of exposure to 10–90 mg/m^3 BPA on estrous cycles and organ histological changes (Chung et al. 2017). There were no neuroendocrine effects induced by BPA exposure in the study by Chung et al. (2017). To say this may be attributed to the fact that BPA levels used in that study which were higher than those shown to induce neuroendocrine effects (National Toxicology Program 2021). A report by the National Toxicology Program showed that ingestion of 2.5 μg/kg BPA influenced neuroendocrine and reproductive function while ingestion of higher concentrations of this chemical (above 250 μg/kg) exerted no marked effect on neuroendocrine/reproductive measures (National Toxicology Program 2021). Modeled estimates of the deposition of BPA in the lungs of animals exposed to 3DP emissions in our study derived an approximately 1.07 μg/kg equivalent dose after 30 days of exposure. Therefore, although the dose and duration of the exposure was lower in the current study than in the other investigations cited,

effects were noted on the neuroendocrine system, and these effects may be associated in part with bisphenols in the 3DP emissions.

It is like that there was accumulation of PM in the nose in this study. It is possible that PM in the olfactory system either chemically or physically interfered with transmission of olfactory cues. Olfactory cues are needed to maintain both reproductive and metabolic function (Dintica et al. 2019; Lumia, Zebrowski, and McGinnis 1987; Kendrick et al. 1997). The mechanism by which inhaled fume components affect central nervous system function is not clear. 3DP emissions may impact the nervous system by directly entering the brain through the nose and olfactory system (Hubbs et al. 2011), or by altering olfactory input to regions of the brain that utilize olfactory information to regulate certain functions. For example, blocking olfactory input inhibits reproductive function (Lumia, Zebrowski, and McGinnis 1987; Powers and Winnans 1973). In the current study, it was found that inhalation of 3DP emissions resulted in a reduction in Mitotracker staining in the olfactory bulb after 1, 8 and 30 day exposure. The reduction in staining is indicative of a decrease in the number of active mitochondria in cells within the olfactory bulb (Buckman et al. 2001; Krajnak 2020; Kudryavtseva et al. 2016; Yu et al. 2016). A change in the number of active cells or in cell function might result in a reduction in olfactory signaling to the brain (Esposti et al. 1999; Kasahara and Scorrano 2014; Kudryavtseva et al. 2016). This alteration in active mitochondria in the olfactory bulb may be attributed to inhalation of PM, or to the estrogenic effects of BPA on mitochondrial function in exposed cells (Yager and Chen 2007). The decrease in Mitotracker staining was also accompanied by a reduction in GDNF and myelin basic protein (MBP) staining. GDNF was shown to be co-localized in myelinating glia Schwann cells and ensheathing cells in the olfactory bulb (Dintica et al. 2019; Kucera et al. 2019; Woodhall, West, and Chuah 2001). As mentioned above, a reduction in myelination of cells that project from the olfactory bulb to the brain may lead to decrease in the transmission of olfactory information and alterations in the transduction of cues that modulate reproductive and metabolic physiology (Baroncini et al. 2007; Lumia, Zebrowski, and McGinnis 1987; Mackay and Abidzaid 2018).

TH immunostaining (neurons and fibers) was also diminished in the olfactory bulb of 3DP emission exposed animals. TH is the rate limiting enzyme in production of dopamine, which is one of the major neurotransmitters used to transmit olfactory cues from the olfactory bulb to the brain (Banerjee et al. 2013; Dluzen, Park, and Kim 2002; Harvey and T Heinbockel 2018; Li et al. 2017). A reduction in TH staining or TH/dopaminergic cells might also be the result of, or associated with, decrease in functional mitochondria number. These findings are consistent with the notion that inhalation of 3DP emissions may interfere with transmission of olfactory information to various regions of the brain and influence the activity of cells regulating reproduction and metabolism in the hypothalamus (Baroncini et al. 2007; Chung et al. 2017; Mackay and Abidzaid 2018).

The PCR data from the olfactory bulb are for the most part consistent with the histological/immunohistological findings. Exposure to 3DP emissions resulted in a reduction in *catalase* transcript levels which was significant 1 and 8 days following exposure. It's possible that the reduction in the antioxidant, catalase, contributed to the rise in oxidative stress, and that

the increase in oxidative stress induced inflammation and cell damage in the olfactory bulb (Kudryavtseva et al. 2016).

Alterations in mitochondria may also have contributed to functional alterations in the myelinating Schwann cells in the olfactory bulb. Schwann cells in the olfactory bulb may be identified by immunostaining for MBP. Myelinating cells regulate a number of functions in the central nervous system. Myelinating cells remove debris after injury and affect neurotransmission by regulating metabolites used in the synthesis of neurotransmitters, and the enzymes that induce the degradation of neurotransmitters. Myelinating cells affect neuronal connectivity by regulating the physical and chemical communication between cells; as well as modulate glucose utilization (LeLoup et al. 2016; Morel et al. 2017). Although olfaction was not measured in the current experiment, changes in (1) myelination of axons, (2) TH immunolabeling, and (3) number of active mitochondria suggest that exposure to 3DP emissions may result in a reduction in olfactory cell function. Changes in olfaction were reported to affect maternal recognition of neonates, the timing of puberty, reproductive behavior, food intake and one trial learning taste aversion (). Alterations in olfaction were also used as an early marker to detect the onset of neurodegenerative diseases (Dintica et al. 2019).

There were also alteration in immunostaining in the hypothalamus. These effects may not be the direct result of PM- or chemical-induced injury to cells, but rather from changes in other regions of the brain that regulate hypothalamic neuronal modulation of endocrine function. For example, no treatment-related effects were observed with either Mitotracker or Fluoro-Jade staining in the hypothalamus, indicating that there were no 3DP emission-related alterations in the hypothalamic mitochondrial levels or neuronal cell injury. However, exposure to 3DP emissions did alter TH and GNRH immunostaining. TH immunostaining increased in both air and 3DP emission exposed animals after 8 day exposure and remained high in the hypothalamus of air-exposed animals after 30 days. However, in 3D-emission treated animals, TH levels were significantly decreased after 30 days. TH immunostaining is seen in dopamine (DA) neurons and fibers and is used to identify DA neurons in the hypothalamus. It also has been used as a marker of DA neuron activity because changes in immunostaining were associated with alterations in the synthesis and release of DA in the hypothalamus (Badasz et al. 2007; Vecchio et al. 2021). More specifically, DA is synthesized and released from the tuberoinfundibular DA (TIDA) neurons in the arcuate and paraventricular nucleus of the hypothalamus, and inhibit release of prolactin and other hormones from the anterior pituitary. In turn, prolactin feedbacks onto TIDA neurons to regulate the release of DA (Freeman et al. 2000). In this study, 8 day treatment elevated immunolabeling for TH and this rise was associated with a reduction in circulating prolactin concentrations in both air and 3DP emission exposed animals. After 30 day exposure prolactin concentrations returned to levels seen with 1 day in air-controls but was significantly decreased in 3DP emission exposed animals. The lower levels of TH immunolabeling (and possibly DA concentrations) noted after 30 day exposure to 3DP emissions might be the result of a longer-term decline in prolactin (Vecchio et al. 2021). TH levels (and DA) levels may have declined to enable prolactin synthesis and release to rise. Changes in TH (or DA synthesis and release) may have also contributed to the observed decrease in circulating TSH concentrations (Connell et al. 1985; Hanew et al. 1991)

There were also changes in hypothalamic GnRH, with exposure to 3DP emissions associated with a significant reduction in GnRH cell number after all treatments. However, GnRH immunostaining did not fall below 1 day levels during the experiment. The decrease in cell number after all exposures, and the reduction in fiber area after 30 day treatment suggests that exposure to 3D printer emissions may have initially induced a rise in the synthesis and release of GnRH which may have stimulated enhanced FSH release. It is possible that a longer duration exposure to printing emissions, or treatment with a higher dose, may have induced a further reduction in GnRH levels and eventually resulted in diminished FSH levels, which subsequently may have contributed to the decrease number of spermatogonium seen after 30 days (Ma et al. 2019; Ullah et al. 2018; Mustieles et al. 2015). There were no significant changes in transcript expression in the hypothalamus (Table 5). It is possible that either the exposure duration was not sufficient, or the dose was not high enough to induce alterations in transcript expression.

Occupational exposures to 3D-printer emissions and bisphenols have been associated with dysfunction of the hypothalamic-pituitary-gonadal and/or thyroid axes in workers (Cimmino et al. 2020; Li et al. 2020; Mustieles et al. 2015; Rochester 2013). We didn't assess These changes were not assessed in the pituitary in the current study; however, circulating concentrations of certain anterior pituitary hormones were determined. There were decreases in circulating concentrations of TSH and prolactin, and significant increases in FSH after 30 days of exposure. The overall reduction in TSH may be attributed to an increase in circulating TH levels. The animals used in this study are between 6 and 8 weeks of age and still undergoing significant growth during this period. Therefore, it is possible that the overall decrease in circulating TSH occurred in response to changes in circulating TH concentrations. The additional fall that was noted in 3D-emission exposed animals may have been associated with effects of exposure on the pituitary or the thyroid. Exposure to BPA during development was found to affect growth and TH levels (National Toxicology Program, 2021). Additional studies examining the influence of inhalation of 3DP emissions on these endocrine glands might aid in determining the underlying mechanism(s) by which inhalation of 3D-printer fume affects TSH and TH concentrations.

FSH concentrations also changed over time, but this change was primarily in air control animals. Following a 1 day treatment, FSH concentrations were below the level of detectability in control animals, and higher in animals exposed to 3DP. However, after 30 day exposure, there was an elevation in FSH in controls, but no marked change in 3DP-exposed animals. The inability to detect FSH in control animals may have been the result of stress where the animals were not familiar with the exposure chamber or the sound of the exposure system. For example, stress-related hormones such as cortisol and corticotropic releasing hormone enhance release of gonadotropins in both males and females (McCosh et al. 2022; Myerhoff et al. 1990). The higher levels of FSH in 3DP exposed animals may be attributed to the estrogenic actions of BPA, which in males stimulates gonadotropin and gamete production (Brouard et al. 2016). Finally, FSH is also a pulsatile hormone and it is possible that a combination of lower overall release of FSH and sampling at the nadir of a pulse, when FSH is lower, led to levels appearing lower in control animals on day 1. The increase in FSH in air controls after 30 days of exposure, may have been due to an acclimation of this hormone in these animals related to the exposure system or age. The

alterations in FSH were not associated with significant changes in estradiol concentration. The effects of exposure on testosterone concentrations were not examined as there was not enough plasma to perform this assay. There are studies that demonstrated that exposure to bisphenols affect testosterone concentrations (Cimmino et al. 2020; Skledar and Masic 2016; Ullah et al. 2018), and thus it is conceivable that circulating testosterone concentrations were also reduced in this experiment. It is of interest that significant changes were detected in Sertoli and Leydig cell number early during the exposure, as well as a longer-term decrease in spermatogonium, suggesting that 3DP emission exposure may lower the number of sperm in males. Additional data needs to be collected to determine if these changes were due to the effects of 3DP emission exposure on the hypothalamus and pituitary, or to the direct effect of 3DP emissions on the testes.

Conclusions

The results of this study are consistent with other data demonstrating that certain plastics used for 3DP may exert effects on the neuroendocrine system by acting at the level of the hypothalamus, and possibly the pituitary and gonads. These alterations are consistent with those of other studies demonstrating that BPA, which is present in 3D emissions generated using polycarbonate plastics, exhibit the potential to act as endocrine disruptors (this study and Stefaniak et al. 2021). However, one cannot rule out the possibility that the effects may have also been due to PM accumulation in various tissues that are part of hypothalamic-pituitary-axis.

There are engineering controls that have been designed to prevent exposures to plastic PM and VOC generated during 3DP. For example, newer, high performance 3D printers include lids and ventilation systems that reduce exposure for the operator. These controls are often seen on printers used in large manufacturing settings. However, less expensive 3D printers that are more likely used in small businesses, homes, and schools often do not possess control strategies used to contain emissions or to remove particles and therefore may pose a hazard (Yi et al. 2016; House, Rajaram, and Tarlo 2017; Stefaniak et al. 2018).

Even if there are ventilation systems to remove the plastic PM from the air, this particulate is often released into the environment where it is deposited in soil and water sources (Raddadi and Fava 2019). There are a number of published studies demonstrating that microplastics, and the chemicals released during their degradation, exert significant effects on the health and development of both humans and aquatic organisms (Burgos-Aceves et al. 2022; Dmytriw 2020; Rubio, Marcos, and Hernandez 2020; Sharma and Chatterjee 2017; Wright and Kelly 2017). The current experiment focused on the effects of 3DP in males because the models for particle deposition were developed in males (Porter et al. 2001). However, females may respond differently because their exposure may be different. Respiratory rate might be affected by a number of factors including age, gender, size of a human or animal or preexisting conditions (Nadziejko et al. 2002; Wallis et al. 2005) and differences in respiration due to these factors may affect the levels and deposition of particulate in the respiratory system. Females may also display different responses and changes in various biomarkers may vary, especially when looking at the effects on the endocrine and neuroendocrine systems. Additional studies need to be conducted to

examine the effects of exposure to 3DP emissions on the endocrine system and on general physiological processes. Additional research better characterizing the potential uptake of these particles in humans and animals, and the rate at which they dissolve in the body is important. Further, knowing which toxicants are contained in various plastics might provide information that may lead to development of plastic polymers that contain fewer substances that might pollute the environment and endanger the health of both humans and wildlife.

Funding

The work was supported by the U.S. Consumer Safety Product Commission [Interagency Agreement with CPSC 61320618H0019]; U.S Consumer Product Safety Commission [Interagency Agreement with CPSC 61320618H0019]; Government Interagency Agreement with CPSC [61320618H0019]; U.S. Consumer Product Safety Commission [Interagency Agreement with CPSC 61320618H0019].

Data availability statement

The data included in this manuscript can be found at Data and Statistics Gateway in the Research Data section: https://www.cdc.gov/niosh/data/researchdata.html

References

Abraham A, and Chakraborty P. 2019. A review on sources and health impacts of bisphenol a. Rev. Environ. Health. doi:10.1515/reveh-2019-0034.

Azimi P, Zhao D, Pouzet C, Crain NE, and Stephens B. 2016. Emissions of ultrafine particles and volatile organic compounds from commercially available desktop three-dimensional printers with multiple filaments. Environ. Sci. Technol. 50 (3):1260–68. doi:10.1021/acs.est.5b04983. [PubMed: 26741485]

Badasz C, Smiley JF, Figarsky K, Saito M, Toth R, Gyetvai BM, Oros M, Kovacs K, Mohan P, and Wang R. 2007. Mesencephalic dopamine neuron number and tyrosine hydroxylase content: Genetic control and candidate genes. Neuro. sci 149 (3):561–72. doi:10.1016/j.neuroscience.2007.06.049.

Baker BA, Mercer RR, Geronilla KB, Kashon ML, Miller GR, and Cultip RG. 2007. Impact of repetition number on muscle performance and histological response. Med. Sci. Sports Exerc. 39 (8):1275–81. doi:10.1249/mss.0b013e3180686dc7. [PubMed: 17762360]

Banerjee K, Akiba Y, Baker H, and Cave JW. 2013 2–13. Epigenetic control of neurotransmitter expression in olfactory bulb interneurons. Int. J. Dev. Neurosci. 31 (6):415–23. doi:10.1016/j.ijdevneu.2012.11.009. [PubMed: 23220178]

Baroncini M, Allet C, Leroy D, Beauvillain JC, Francke JP, and Prevot V. 2007. Morphological evidence for direct interaction between gonadotrophin-releasing hormone neurones and astroglial cells in the human hypothalamus. J. Neuroendocrinol. 19 (9):691–702. doi:10.1111/j.1365-2826.2007.01576.x. [PubMed: 17680884]

Brouard V, Guenon I, Bouraima-Lelong H, and Delalande C. 2016. Differential effects of bisphenol a and estradiol on rat spermatogenesis establishement. Reprod. Toxicol. 63:49–61. doi:10.1016/j.reprotox.2016.05.003. [PubMed: 27174447]

Buckman JF, Hernandez H, Kress GJ, Votyakova TV, Pal S, and Reynolds IJ. 2001. Mitotracker labeling in primary neuronal and astrocytic cultures: Influence of mictochondrial membrane potential and oxidants. J. Neurosci. Meth. 104 (2):165–76. doi:10.1016/S0165-0270(00)00340-X.

Burgos-Aceves MA, Faggio C, Betancourt-Lozano M, Gomzalez-Mille DJ, and Llizaliturri-Hernandez CA. 2022. Ecotoxicological perspectives of microplastic pollution in amphiphians. J. Toxicol. Environ. Health 25 (8):405–21. doi:10.1080/10937404.2022.2140372.

Catenza CJ, Farooq A, Shubear NS, and Donkor KK. 2021. A targeted review on fate, occurrence, risk and health implications of biphenol analogues. Chemosphere 268:129273. doi:10.1016/j.chemosphere.2020.129273. [PubMed: 33352513]

Chan FL, Chan FL, Hon CY, Tarlo SM 2020. Emissions and health risks from the use of 3D printers in an occupational setting. J. Toxicol. Environ Health, Part A 83 (7):279–87. doi:10.1080/15287394.2020.1751758.

Chung YH, Han JY, Lee SB, and Lee YH. 2017. Inhalation toxicity of bisphenol a and its effect on estrous cycle, spatial learning, and memory in rats upon whole-body exposure. Toxicol. Res. 33 (2):165–71. doi:10.5487/TR.2017.33.2.165. [PubMed: 28503266]

Cimmino I, Fiory F, Perruolo G, Miele C, Beguinot F, Formisano P, and Oriente F. 2020. Potential mechanisms of bisphenol a (BPA) contributing to human disease. Int. J. Mol. Sci 21 (16):5761. doi:10.3390/ijms21165761. [PubMed: 32796699]

Connell JM, Ball SG, Balmforth AJ, Beastall GH, and Davies DL. 1985. Effect of low-dose dopamine infusion on basal and simulated TSH and prolactin concentrations in man. Clin. Endocrinol. 23 (2):185–92. doi:10.1111/j.1365-2265.1985.tb00214.x.

Dintica CS, Marseglia A, Rizzuto D, Want R, Afranakis J, Seubert K, Bennet DA, and Xu W. 2019. Impaired olfaction is associated with cognitive decline and neurodegeneration in the brain. Neurol 92 (7):e701–e09. doi:10.1212/WNL.0000000000006919.

Dluzen DE, Park J-H, and Kim K. 2002. Modulation of olfactory bulb tyrosine hydroxylase and catecholamine transporter mRN by estrogen. Mol. Brain. Res. 108 (1–2):121–28. doi:10.1016/S0169-328X(02)00520-X. [PubMed: 12480184]

Dmytriw AA 2020. The microplastics menace: An emerging link to environment and health. Sci. Total Environ. 707:135558. doi:10.1016/j.scitotenv.2019.135558. [PubMed: 31761361]

Esposti MD, Hatzinisiriou I, McLennan H, and Ralph S. 1999. Bcl-2 and mitochondrial oxygen radicals. New approaches with reactive oxygen species-sensitive probes. J. Biol. Chem. 274 (42):29831–37. doi:10.1074/jbc.274.42.29831. [PubMed: 10514462]

Farcas MT, McKinney W, Qi C, Mandler KW, Battelli L, Friend SA, Stefaniak AB, Jackson M, Orandle M, Winn A, Kashon M, et al. 2020. Pulmonary and systemic toxicity in rats following inhalation exposure of 3-D printer emissions from acrylonitrile butadiene styrene (ABS) filament. Inhal. Toxicol 32 (11–12):403–18. doi:10.1080/08958378.2020.1834034. [PubMed: 33076715]

Farcas MT, Stefaniak AB, Knepp AK, Bowers L, Mandler WK, Kashon M, Jackson SR, Stueckle TA, Sisler JD, Friend SA, Qi C et al. 2019. Acrylonitrile butadiene styrene (ABS) and polycarbonate (PC) filaments three-dimensional (3-D) printer emissions-induced cell toxicity. Toxicol. Lett. 317:1–12. doi:10.1016/j.toxlet.2019.09.013. [PubMed: 31562913]

Freeman ME, Kanyucska B, Lerant A, and Nagy G. 2000. Prolactin: Structure, function and regulation secretion. Physiol. Rev. 80 (4):1523–631. doi:10.1152/physrev.2000.80.4.1523. [PubMed: 11015620]

Hanew K, Utsumi A, Sugawara A, Shimizu Y, and Yoshinaga K. 1991. Evidence for dopamine-related and TRH-related pituitary TSH and PRL pools in patients with prolactinoma. Acta Endocrinol. 124 (5):545–542. doi:10.1530/acta.0.1240545.

Harvey JD, and T Heinbockel T. 2018. Neuromodulation of synaptic transmission in the main olfactory bulb. Int. J. Environ. Res. Pub Health 15 (10):2194. doi:10.3390/ijerph15102194. [PubMed: 30297631]

House R, Rajaram N, and Tarlo SM. 2017. Case report of asthma associated with 3D printing. Occup. Med. 67 (8):652–54. doi:10.1093/occmed/kqx129.

Hubbs AF, Mercer RR, Benkovic SA, Harkema J, Sriram K, Schwegler-Berry D, Goravanahally MP, Nurkiewicz TR, Castranova V, and Sargent LM. 2011. Nanotoxicology—A Pathologist's Perspective. Toxicol. Pathol 39 (2):301–24. doi:10.1177/0192623310390705. [PubMed: 21422259]

Johnson C, Miller GR, Baker BA, Hollander M, Kashon ML, Waugh S, and Krajnak K. 2016. Changes in the expression of calcitonin gene-related peptide after exposure to injurious stretch shortening contactions. Exp. Genontol 15:1–7. doi:10.1016/j.exger.2016.03.006.

Kasahara A, and Scorrano L. 2014. Mitochondria: From cell death executioners to regulators of cell differentiation. Trends Cell Biol. 24 (12):761–70. doi:10.1016/j.tcb.2014.08.005. [PubMed: 25189346]

Kendrick KM, Da Costa APC, Broad KD, Ohkura S, Guevara R, Lévy F, and Keverne EB. 1997. Neural control of maternal behaviour and olfactory recognition of offspring Brain Res Bull. Brain Res. Bull. 44 (4):383–95. doi:10.1016/S0361-9230(97)00218-9. [PubMed: 9370203]

Kim Y, Yoon C, Ham S, Park J, Kim S, Kwon O, and Tsai PJ. 2015. Emissions of nanoparticles and gaseous material from 3D printer operation. Environ. Sci. Technol. 49 (20):12044–53. doi:10.1021/acs.est.5b02805. [PubMed: 26402038]

Krajnak K 2020. Frequency-dependent changes in mitochondrial number and generation of reactive oxygen species in a rat model of vibration-induced injury. J. Toxicol. Environ. Health Part A 83 (1):20–35. doi:10.1080/15287394.2020.1718043.

Krajnak K, Waugh S, Johnson C, Miller GR, Xu X, Warren C, and Dong RG. 2013. The effects of impact vibration in peripheral blood vessels and nerves. Ind. Health 51 (6):572–80. doi:10.2486/indhealth.2012-0193. [PubMed: 24077447]

Kucera J, Ruda_kucerova J, Zlamal F, Kurucova D, Babinska Z, Tomandl J, Tomandlova M, and Vienertiva-Vasku J. 2019. Oral administration of BDNF and or GDNF normalizes serum BDNF level in the olfactory bulbectomized rats: A proof of concept study. Pharmacol. Rep 71 (4):669–75. doi:10.1016/j.pharep.2019.03.005. [PubMed: 31195344]

Kudryavtseva AV, Krasnov GS, Dmitriev AA, Alekseev BY, Kardymon OL, Sadritdinova AF, Fedorova MS, Pokrovsky AV, Melnikova NV, and Kaprin AD. 2016. Mitochondrial Dysfunction and oxidative stress in aging and cancer. Oncotarget 7 (29):44879–905. doi:10.18632/oncotarget.9821. [PubMed: 27270647]

Lehmler H, Liu J, Gadogbe B, and Bao W. 2018. Exposure to Bisphenol A, Bisphenol F, and Bisphenol S in U.S. Adults and Children: The National Health and Nutrition Examination Survey 2013–2014. ACS. Omega 3 (6):6523–32. doi:10.1021/acsomega.8b00824. [PubMed: 29978145]

LeLoup C, Allard C, Carniero L, Fiormonte X, Collins S, and Nicaud LP. 2016. Glucose and hypothalamic astrocytes: More than a fueling role? Neuro. sci 323:110–20. doi:10.1016/j.neuroscience.2015.06.007.

Leso V, Ercolano ML, Mazzotta I, Romano M, Cannavacciuolo F, and Iavicoli I. 2021. Three-dimensional (3D) printing: Implications for risk assessment and management in occupational settings. Ann. Work Exp. Health 2021 (6):617–34. doi:10.1093/annweh/wxaa146.

Li Y, Want Y, Guo L, Lei L, and Wang D. 2017. Effects of pinealectomy and gonadectomy on olfactory bulb dopaminergic neurons in rats. Chinese. Med. J 11130:2302–06.

Li X, Wen Z, Wang Y, Mo J, Zhong Y, and Ge RS. 2020. Bisphenols and Leydig cell development. Front. Endocrinol. 31. doi:10.3389/fendo.2020.00447.

Lumia AR, Zebrowski AF, and McGinnis MY. 1987. Olfactory bulb removal decreases androgen receptor binding in amygdala and hypothalamus and disrupts manscular sexual behavior. Brain Res. 404 (1–2):121–26. doi:10.1016/0006-8993(87)91362-X. [PubMed: 3567559]

Mackay H, and Abidzaid A. 2018. A plurality of molecular targets: The receptor ecosystem for bisphenol-A (BPA). Horm. Behav 101:59–67. doi:10.1016/j.yhbeh.2017.11.001. [PubMed: 29104009]

Ma Y, Liu H, Wu J, Yuan L, Wang Y, Du X, Want R, Marwa PW, Petlulu P, Chen X, et al. 2019. The adverse health effects of bisphenol a and related toxicity mechanisms. Environ. Res. 176:108575. doi:10.1016/j.envres.2019.108575. [PubMed: 31299621]

Martín CM, Blettler A, Elie A, Farhan R, Khan B, Nuket S, and Luis AE. 2018. Freshwater plastic pollution: Recognizing research biases and identifying knowledge gaps. Water Res. 143:416–24. doi:10.1016/j.watres.2018.06.015. [PubMed: 29986250]

McCosh RB, O'Bryne KT, Karsch FJ, and Breen KM. 2022. Regulation of the gonadotropin-releasing hormone neuron during stress. J. Neuroendocrinol. 34 (5):e13098. doi:10.111/jne.13098. [PubMed: 35128742]

Morel L, Chiang M-S, Higashimori H, Shoneye T, Lyer LK, Yelick Y, Tai T, and Yang Y. 2017. Molecular and functional properties of regional astrocytes in the adult brain. J. Neurosci. 37 (36):8706–17. doi:10.1523/JNEUROSCI.3956-16.2017. [PubMed: 28821665]

Mustieles V, Pérez-Lobato R, Olea N, and Fernandez M. 2015. Bisphenol A: Human exposure and neurobehavior. Neuro. Toxicol 49:174–84. doi:10.1016/j.neuro.2015.06.002.

Myerhoff JL, Oleshanksy MA, Kalogeras KT, Mougey EH, Chrousos GP, and Granger LG. 1990. Neuroendocrine responses to emotional stress: Possible interactions between circulating factors and anterior pituitary hormone release. Adv. Exp. Med. Biol. 274:91–111. [PubMed: 2173366]

Nadziejko C, Fang K, Nadziejko E, Narciso SP, Zhong M, and Chen LC. 2002. Immediate effects of particulate air pollutants on heart rate and respiratory rate in hypertensive rats. Cardiovas Toxicol. 2 (4):245–52. doi:10.1385/CT:2:4:245.

National Insitute for Occupational Safety and Health. 2018. Volatile organic compounds, C1 to C10, canister method, 3900. NIOSH Manual of Analytic Methods (NMAM), edited by N. I. f. O. S. a, Washinton DC, USA: Health.

National Toxicology Program. 2021. NTP research report on the consortium linking academic and regulatory insights on bisphenol a toxicity (CLARITY-BPA): A compendium of published findings. Research Triangle Park, North Carolina.

Persaud K 2013. Engineering aspects of olfaction. In Frontiers in neuroengineering, eds. Persaud KC, Marco S, and Guitierrez-Galvez A, pp. 1–58. Boca Raton, FL: CRC Press/Taylor & Francis. doi:10.1201/b14670-2

Porter DW, Ramsey D, Hubbs AF, Batelli L, Ma J, Barger M, Landsittel D, Robinson VA, McLaurn J, Khan A, et al. 2001. Time course of pulmonary responses of rats to inhalation of crystalline silica: Histological results and biomchemical indices of damage, lipidosis, and fibrosis. J. Environ. Pathol. Toxicol. Oncol. 20 (1):1–14. doi:10.1615/JEnvironPatholToxicolOncol.v20.iSuppl.1.10.

Powers JB, and Winnans SS. 1973. Sexual behavior in perpherally ansosmic male hamsters. Physiol. Behav. 10 (2):361–68. doi:10.1016/0031-9384(73)90323-5. [PubMed: 4736134]

Raddadi N, and Fava F. 2019. Biodegradation of oil-based plastics in the environment: Existing knowledge and needs of research and innovation. Sci. Total Environ. 679:148–58. doi:10.1016/j.scitotenv.2019.04.419. [PubMed: 31082589]

Roberts JR, Anderson SE, Kan H, Krajnak K, Thompson JA, Kenyon A, Goldsmith WT, McKinney W, Frazer DG, Jackson M, et al. 2014. Evaluation of pulmonary and systemic toxicity of oil dispersant (COREXIT EC9500A((R) following cute repeated inhalation exposure. Environ. Health Insights 8 (Suppl 1):63–74. doi:10.4137/EHI.S15262. [PubMed: 25861220]

Rochester JA 2013. Bisphenol a and human health: A review of the literature. Reprod. Toxicol. 42:132–55. doi:10.1016/j.reprotox.2013.08.008. [PubMed: 23994667]

Rubio L, Marcos R, and Hernandez A. 2020. Potential adverse health effects of ingested micro- and nanoplastics on humans. Lessons learned from in vivo and in vitro mammalian models. J. Toxicol. Environ. Health B 23 (2):51–68. doi:10.1080/10937404.2019.1700598.

Sharma S, and Chatterjee S. 2017. Microplastic pollution, a threat to marine ecosystem and human health: A short review. Environ. Sci. Pollut. Res. 24 (27):21530–47. doi:10.1007/s11356-017-9910-8.

Skledar DG, and Masic LJ. 2016. Bisphenol a and its analogs: Do their metabolites have endocrine activity? Environ. Toxicol. Pharmacol. 47:182–99. doi:10.1016/j.etap.2016.09.014. [PubMed: 27771500]

Slotnick B, and Coppola DM. 2015. Odor-cued taste avoidance: A simple and robust test of mouse olfaction. Chem. Senses 40 (4):269–78. doi:10.1093/chemse/bjv005. [PubMed: 25787943]

Stefaniak AB, Bowers LN, Knepp AK, Virji AM, Birch EM, Ham JE, Wells JR, Chaolong Q, Schwegler-Berry D, Friend S, et al. 2018. Three-dimensional printing with nano-enabled filaments releases polymer particles containing carbon nanotubes into air. Indoor Air 28 (6):840–51. doi:10.1111/ina.12499. [PubMed: 30101413]

Stefaniak AB, Bowers LN, Martin SB, Hammond DR, Ham JE, Wells JR, Fortner AR, Knepp AK, du Preez S, Pretty JR, et al. 2021. Large-format additive manufacturing and machining using high-melt-temperature polymers. ACS Chem. Health Saf 26 (4):268–78. doi:10.1021/acs.chas.0c00129.

Stefaniak AB, LeBouf RF, Duling MG, Yi J, Abukabda AB, McBride CR, and Nurkiewicz TR. 2017. Inhalation exposure to three-dimensional printer emissions stimulates acute hypertension and microvascular dysfunction. Toxicol. App. l Pharmacol 335:1–5. doi:10.1016/j.taap.2017.09.016.

Suhyun P, Yeongwan H, Jiyun L, Younglim K, and Kyunghee J. 2019. Chronic effects of bisphenol S and bisphenol SIP on freshwater waterflea and ecological risk assessment. Ecotoxicol. Environ. Saf 185:109694. doi:10.1016/j.ecoenv.2019.109694. [PubMed: 31562998]

Ullah A, Madeeha P, Sarwat J, Hizb U, Naheed T, Waheed U, Mariyam FS, Muhammad Z, Kinza ZL, and Muhammad MK. 2018. Impact of low-dose chronic exposure to bisphenol a and its analogue bisphenol B, bisphenol F and bisphenol S on hypothalamo-pituitary testicular activities in adult rats: A focus on the possible hormonal mode of action. Food Chem. Toxicol. 121:24–36. doi:10.1016/j.fct.2018.08.024. [PubMed: 30120946]

Vaisanen A, Alonen L, Ylonen S, and Hyttinen M. 2022. Organic compound and particulate emissions of additive manufacturing with photopolymer resins and chemical outgassing of manufactured resin products. J. Toxicol. Environ. Health Part A 85 (5):198–216. doi:10.1080/15287394.2021.1998814.

Vandenburgh JG 1973. Effects of central and peripheral anosmia on reproduction of female mice. Physiol. Behav. 10 (2):257–61. doi:10.1016/0031-9384(73)90307-7. [PubMed: 4708495]

Vasiljevic T, and Harner T. 2021. Bisphenol a and its analogues in outdoor and indoor air: Properties, sources and global levels. Sci. Total Environ. 789:1–16. doi:10.1016/j.scitotenv.2021.148013.

Vecchio LM, Sullivan P, Dunn AR, Bermejo MK, Fu R, Masoud ST, Gregersen E, Urs NM, Nazari R, Jensen PH, et al. 2021. Enhanced tyrosine hyrdoxylase activity induces oxidative stress, causes accumulation of autotoxic catecholamine metabolites, and augments amphetamine effects in vivo. J. Neurochem. 158 (4):960–79. doi:10.1111/jnc.15432. [PubMed: 33991113]

Wallis LA, Healy M, Undy MB, and Maconochie I. 2005. Age related reference ranges for respiration rate and heart rate for 4 to 16 years. Arch. Dis. Child. 90 (11):1117–21. doi:10.1136/adc.2004.068718. [PubMed: 16049061]

Williams GM, Kobets T, Duan JD, Iatropoulos M.J. 2017. Assessment of DNA binding and oxidative DNA damage by acrylonitrile in two rat target tissues of carcinogenicity: Implications for the mechanism of action. Chem. Res. Toxicol. 30 (7):1470–80. doi:10.1021/acs.chemrestox.7b00105. [PubMed: 28613844]

Woodhall E, West AK, and Chuah ME. 2001. Cultured olfactory ensheathing cells expression nerve growth factor, brain-derived neurotrophic factor, glia cell line-derived neurotrophic factor and their receptors. Mol. Brain. Res. 88 (1–2):201–13. doi:10.1016/S0169-328X(01)00044-4.

Wright SL, and Kelly KJ. 2017. Plastic and human health: A microissue. Environ. Sci. Technol. 51 (12):6634–47. doi:10.1021/acs.est.7b00423. [PubMed: 28531345]

Wu H, Fahy WP, Kim S, Kim H, Zhao N, Pilato L, Kafi A, Bateman S, Koo JH 2020. Recent developments in polymers/polymer nanocomposites for additive manufacturing. Prog. Mater. Sci 111:100638. doi:10.1016/j.pmatsci.2020.100638.

Yager J, and Chen JQ. 2007. Mitochondrial estrogen receptors – new insights into specific functions. Trends Endocrinol. Metab. 18 (3):89–91. doi:10.1016/j.tem.2007.02.006. [PubMed: 17324583]

Yi J, LeBouf RF, Duling MG, Nurkiewicz T, Chen BT, Schwegler-Berry D, Virji MA, and Stefaniak AB. 2016. Emission of particulate matter from a desktop three-dimensional (3D) printer. J. Toxicol. Environ. Health Part A 79 (11):453–65. doi:10.1080/15287394.2016.1166467.

Yu B, Wenjun Z, Changsheng Y, Yuntao F, Jing M, Ben L, Hai Q, Guangwei X, Suhua W, Fang L, et al. 2016. Preconditioning of endoplasmic reticulum stress protects against acrylonitrile-induced cytotoxicity in primary rat astrocytes: The role of autophagy. Neurotoxicol 55:112–21. doi:10.1016/j.neuro.2016.05.020.

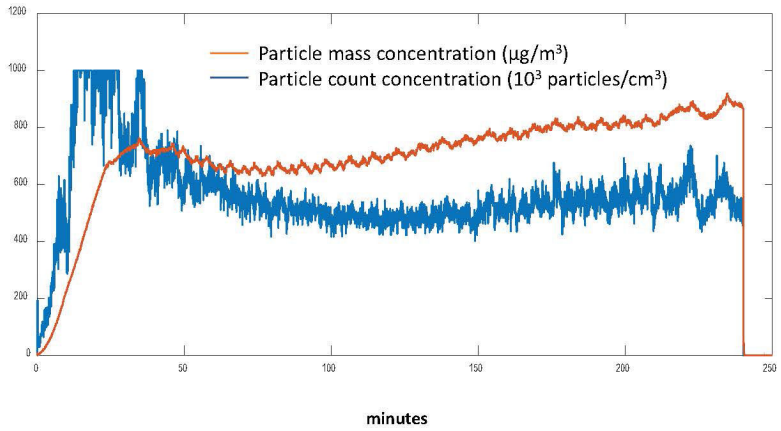

Figure 1.

Chamber particle characterizations. Particle mass concentration (red line) and particle count concentration (blue line) vs time during a single 4 hr exposure.

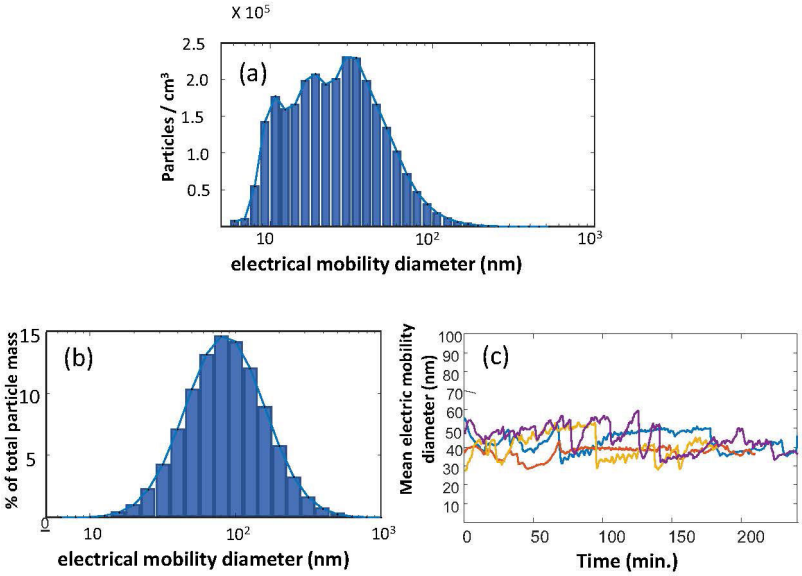

Figure 2.

Particle size measures. (a) Electrical mobility equivalent diameter (FMPS) size reading from the exposure chamber during printing (particle count based size distribution); (b) Particle size distribution from (a) converted to mass assuming all particles were spherical and had a density of 1 g/cm^3; (c) Particle mean electric mobility diameter vs time during four different 4- hour exposures.

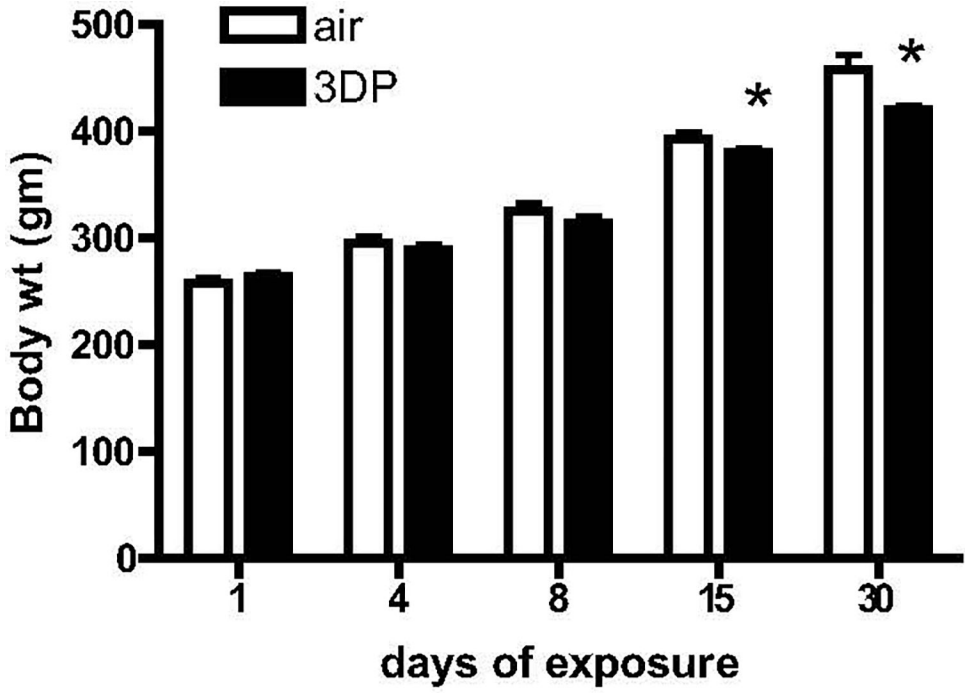

Figure 3.

Body weights in rats exposed to 1, 4, 8, 15 or 30 days of air or 3DP emissions. Animals exposed to 3DP emissions for 15 and 30 days had lower body weights than air controls (*significant, $p < 0.05$).

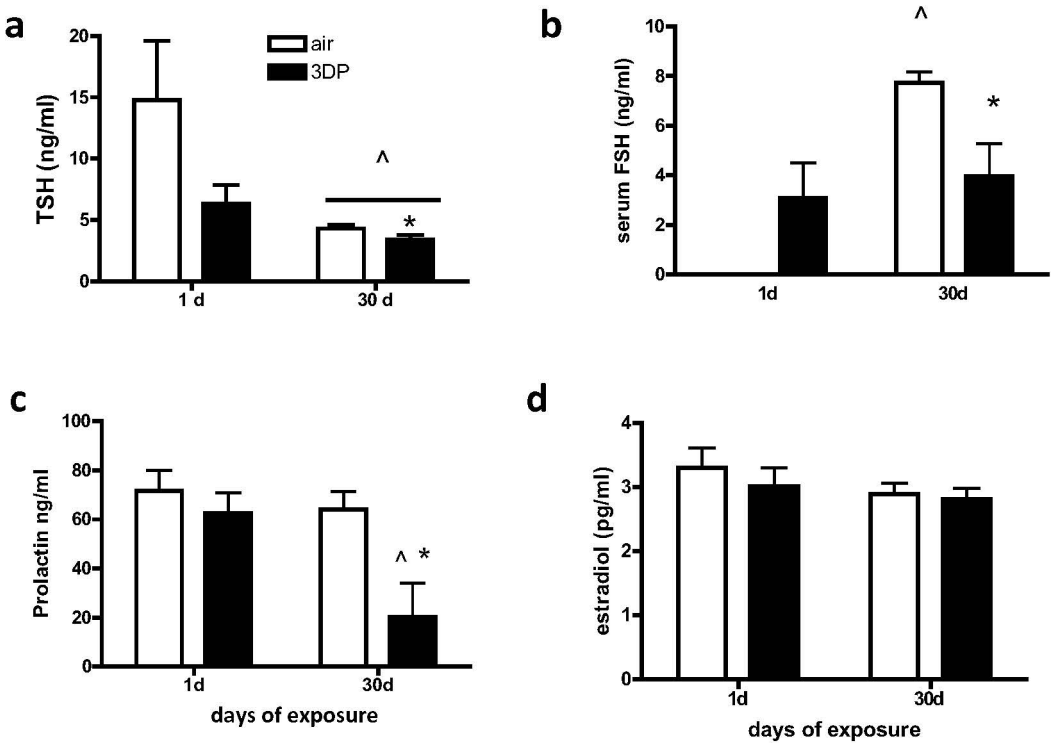

Figure 4.

Average plasma hormone concentrations. Average circulating TSH concentrations were lower after 30 day exposure to both air and 3DP emissions, with concentrations in animals exposed to 3DP emissions lower than air controls after exposure (a). Average circulating FSH concentrations were undetectable in control animals after 1 day exposure, but increased in air control animals after 30d of exposure. FSH concentrations in 3DP emission exposed animals did not change over time, but were lower than air control animals at 30 days (b). Average circulating prolactin concentrations in 3DP emission exposed animals were lower at 30 days compared to 1day air exposed and 1day emission exposed animals (c). Average circulating estradiol concentrations did not change over time or between exposures (d). ^ significantly different than 1 day, $p < 0.05$, *significantly different than same day air controls, $p < 0.05$.

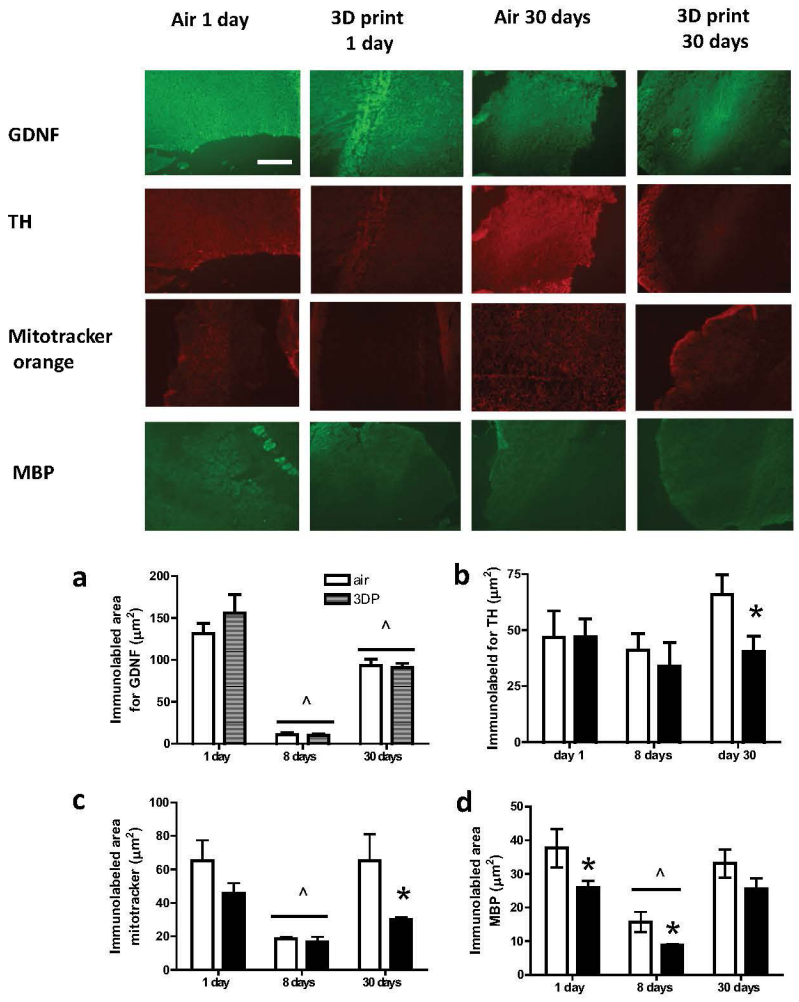

Figure 5.

Photomicrographs of the olfactory bulb after 1 or 30 day exposure and graphs showing the %of the total area immunolabeled (± sem) in the olfactory bulb at 1, 8 and 30 day after exposure. Exposure to air and 3DP emissions resulted in a reduction in GDNF immunolabeling 8 and 30 day following exposure as compared to 1 day after exposure (a). The area of the olfactory bulb immunolabeled for TH generally did not change over the exposures but was lower than air controls in 3DP emissions exposed animals after 30 days exposure (b). The area labeled for Mitotracker orange was significantly lower 8d after exposure to air or 3DP emissions. However, by 30day, labeling returned to 1day levels in air controls, but remained reduced in 3DP emission exposed as compared to air exposed (c). Myelin basic protein (MBP) immunolabeling was reduced 1 and 8 day after exposure to 3DP emissions; both air and 3DP emission exposed animals had lower levels of MBP immunostaining at 8d compared to 1 day exposure groups. By 30day, MBP immunolabeling was returning to 1day levels (d). ^ significantly different than 1d, $p < 0.05$, *significantly different than same day air controls, $p < 0.05$. Bar is 100 μm.

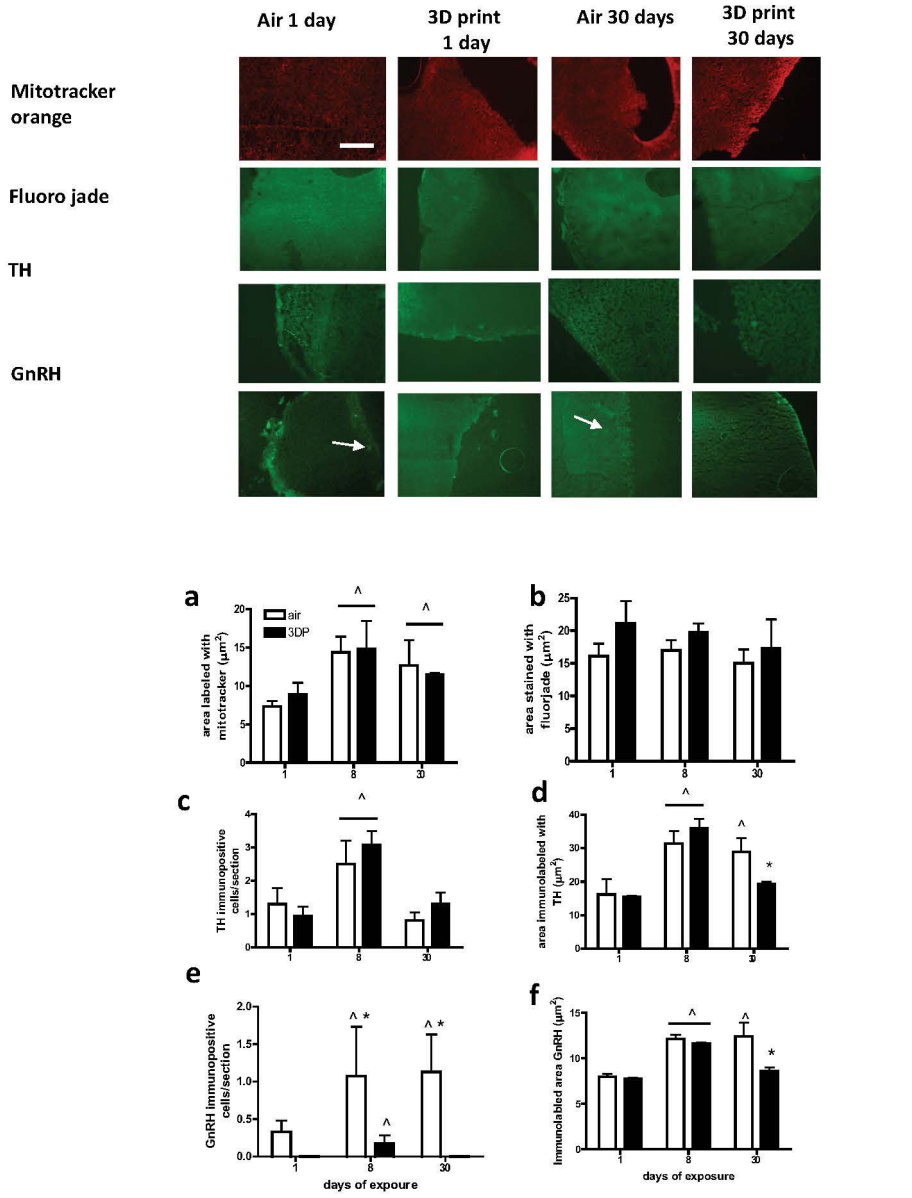

Figure 6.

Photomicrographs of the hypothalamus after 1 or 30 day exposure and graphs showing the % area immunolabeled in the hypothalamus 1, 8 and 30 day after exposure. The area stained with Mitotracker orange was significantly increased 8 and 30 day after exposure to air and 3DP emissions (a). Fluoro-Jade staining, a marker of neuronal injury, did not change in any treatment group over the length of the experiment (b). The number of tyrosine hydroxylase (TH) immunolabeled cells/section was increased 8 day after exposure to both air and 3DP emissions, but returned to 1day levels after 30 day exposure (c). The area immunolabeled (including neurons and fibers) with TH was significantly increased after 8 day exposure in both air and 3DP emission exposed animals. TH immunostaining remained elevated in air controls, but was lower in 3DP emission exposed animals than air controls after 30 day exposure (d). The number of gonadotropin releasing hormone (GnRH) immunolabeled

neurons was higher in air controls at 8 and 30 day after exposure compared to 1day neuron numbers. The number of GnRH neurons was significantly lower in 3DP-exposed animals as compared to air controls 8 and 30 day after exposure (e). GnRH immunolabeled fibers were increased after 8 day exposure to air and 3DP emissions compared to 1day levels. GnRH immunolabeled areas remained high after 30 day exposure to air, but declined after 30 day exposure to 3DP emissions. ^ significantly different than 1 day, $p < 0.05$, *significantly different than same day air controls, $p < 0.05$. Bar is 100 μm.

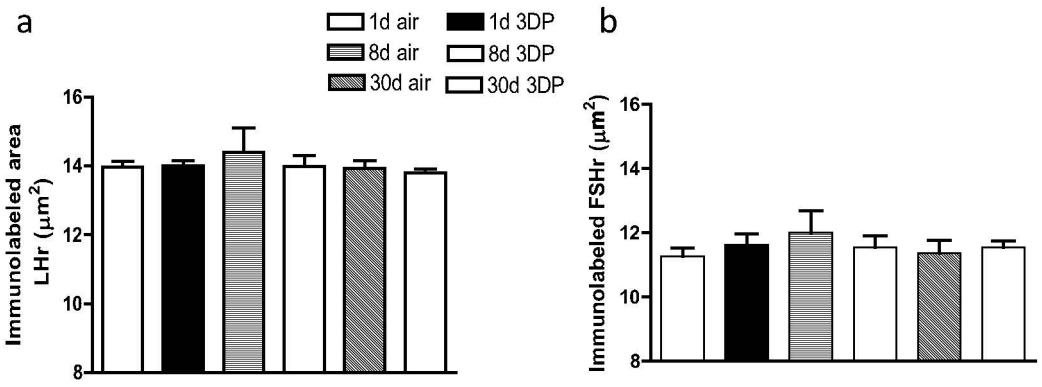

Figure 7.

The area immunolabeled for luteinizing hormone (LH) receptor (LHr; A) and follicle stimulating hormone FSH receptors (FSHr; B) in the testes did not change over the course of the exposure in air or 3DP-emission treated animals.

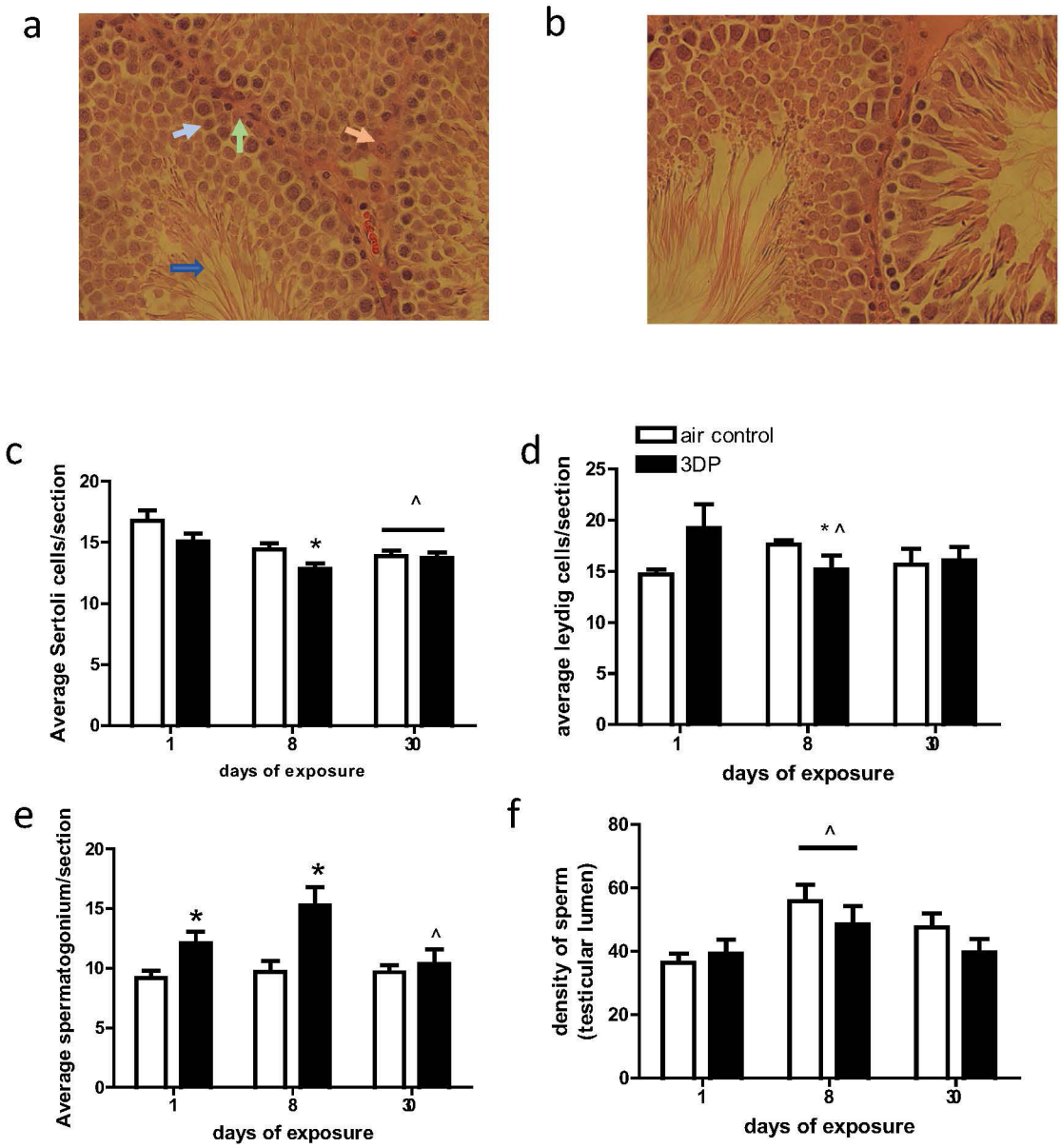

Figure 8.

The photomicrographs at the top of the figure show H&E labeled testes from an air control (a) and 3DP emission (b) exposed animal 30 day after exposure. The graphs show the number of various cell types in the testes determined using stereological procedures. The average number of Sertoli cells/section (c; and green arrows in a) was lower in 3DP emission exposed than air-exposed animals after 8 day, and Sertoli cell number was reduced in both air and 3DP exposed animals 30 day after exposure. Leydig cell (d and orange arrow in a) number was lower in 3DP exposed than air control animals 8 day after exposure, as well as lower than the 1d 3DP emission group. The average number of spermatogonium/section (e and light blue arrow in a) decreased for both treatment groups through the time course of exposures. After 30 day exposure to 3DP emissions, spermatogonium numbers were lower than they were after 1 day as well as to same day air controls. The density of sperm in the

testicular lumen (f and dark blue arrow in a) was higher at 8 day after exposure to air or 3DP emissions than after 1 day exposure. After 30 day exposure, sperm density returned to 1day levels. ^ significantly different than 1 day, $p < 0.05$, *significantly different than same day air controls, $p < 0.05$.

Table 1.

Printer settings used to generate exposure conditions used in this study.

Printer Settings:	Value
Print nozzle temperature	290°C
Print bed temperature	120°C
Layer Height	0.20 mm
Line Width	0.5 mm
Wall thickness	3 lines (1.5 mm)
Number of solid bottom layers	4 (0.8 mm)
Number of solid top layers	4 (0.8 mm)
Infill density	20%
Print speed (1st layer)	30 mm/sec
Print speed after 1st layer	60 mm/sec
Print bed adhesion	Glass bed with PC layer *.

* 40 g of PC filament was dissolved in an acetone solution (100 ml). A thin layer of this solution was brushed onto each glass print bed the day before a print was conducted. The acetone would evaporate, and the vapor flushed out of the print chamber before exposures.

Table 2.

Chemicals measured in emissions collected during 4 h of 3D-printing with polycarbonate stock. Measures were collected on three separate days and the mean concentrations along with standard deviation (std) are reported. OSHA permissible exposure limits (PEL) in parts per billion (PPB) are also listed. None of the chemicals were near or above the PEL. Acetone is not part of the plastic; concentrations in the emissions are a result of acetone used for print bed adhesion.

Compound	mean	SD	OSHA PEL (in ppb)
2,3-Butanedione	<0.3	0	na
2,3-Hexanedione	<0.4	0.00	na
Acetone	1,573.8	1,431.47	1,000,000
Acetonitrile	1.0	0.35	40,000
Benzene	1.0	0.15	1,000
Chloroform	<0.1	0.00	50,000
D-Limonene	2.5	0.42	na
Ethanol	22.4	2.39	1,000,000
Ethylbenzene	<0.3	0.00	100,000
Isopropyl Alcohol	13.6	4.12	400,000
Methyl Methacrylate	2.0	1.22	100,000
Methylene Chloride	<0.2	0.00	25,000
Styrene	2.7	0.44	100,000
Toluene	<0.3	0.00	200,000
alpha-Pinene	<0.5	0.00	na
m,p-Xylene	1.5	0.25	100,000
n-Hexane	<0.4	0.00	500,000
o-Xylene	1.2	0.20	100,000

Table 3.

Antibodies and stains used to identify proteins, receptors or structures, the vendor it was purchased from and the final dilution.

Primary antibody	Vendor	dilution
Mouse anti-follicle stimulating hormone receptor (FSHr)	Santa Cruz Antibodies	1:250
Mouse anti-glial-derived neurotrophic factor (GDNF)	Santa Cruz Antibodies	1:500
Mouse anti-gonadotropin releasing hormone (GnRH)	Santa Cruz Antibodies	1:500
Mouse anti-luteinizing hormone receptor (LHr)	Santa Cruz Antibodies	1:500
Mouse anti-tyrosine hydroxylase (TH)	Santa Cruz Antibodies	1:500
Mouse anti-myelin basic protein (MBP)	Santa Cruz Antibodies	1:250
Goat anti-mouse Cy3 or Fluorescein	Jackson Immunolabs	1:800
Mitotracker (stain)	Invitrogen	500 nm final dilution
Fluoro-Jade C (stain)	Sigma	1:10,000 final dilution

Table 4.

Fold changes in transcript expression in the olfactory bulb of animals exposed to air or 3D printer emissions after 1, 4, 8, 15, or 30 days of exposure.

	Olfactory bulb				
transcripts	**1 day**	**4 days**	**8 days**	**15 days**	**30 days**
c-Fos air	1.63 (0.68)	1.10 (0.23)	1.30 (0.32)	1.03 (0.11)	1.44 (0.41)
3-D emissions	1.05 (0.35)	**0.53 (0.08)** *	0.79 (0.15)	1.28 (0.19)	**2.48 (0.55)** ^
Cat air	1.03 (0.13)	1.08 (0.17)	1.07 (0.17)	1.18 (0.36)	1.09 (0.23)
3-D emissions	**0.58 (0.15)** *	**0.77 (0.14)** *	**0.70 (0.08)** *	**0.73 (0.08)** *	**0.76 (0.07)** *
Gdnf air	1.49 (0.46)	2.58 (1.71)	1.17 (0.29)	1.66 (0.94)	2.98 (0.81)
3-D emissions	**0.44 (0.19)** *	3.14 (1.19)	**2.57 (0.63)** *	1.41 (0.38)	2.87 (0.44)
Gfap air	1.22 (0.42)	0.87 (0.22)	2.38 (0.40)	1.27 (0.15)	0.88 (0.15)
3-D emissions	1.42 (0.72)	2.13 (0.56))	2.12 (0.31)	1.06 (0.20)	1.44 (0.16)
Il1β air	1.16 (0.32)	1.03 (0.13)	1.10 (0.24)	1.13 (0.26)	1.11 (0.24)
3-D emissions	1.09 (0.26)	1.29(0.34)	1.12 (0.14)	1.87 (0.65)	0.97 (0.83)
Il6 air	1.00 (0.42)	1.44 (0.41)	1.49 (0.56)	2.28 (1.155)	1.23 (0.34)
3-D emissions	4.06 (2.20)	5.46 (2.61)	1.81 (0.75)	1.92 (0.85)	1.51 (0.69)
Sod2 air	1.01 (0.10)	0.94 (0.08)	0.97 (0.12)	1.08 (0.18)	1.09 (0.19)
3-D emissions	1.00 (0.08)	0.88 (0.09)	0.92 (0.05)	0.86 (0.04)	1.20 (0.14)
Tnf-α air	1.02 (0.11)	1.06 (0.08)	1.11 (0.16)	1.09 (0.19)	1.32 (0.14)
3-D emissions	1.40 (0.42)	1.51 (0.18)	1.34 (0.15)	**2.31 (0.30)** *	1.69 (0.23)
Vim air	1.22 (0.27)	1.24 (0.38)	1.19 (0.32)	1.98 (1.08)	1.36 (0.14)
3-D emissions	0.85 (0.19)	0.96 (0.27)	0.79 (0.09)	2.14 (0.81)	1.34 (0.52)

The numbers that are bold* are significantly different than air controls on that day and the numbers that are only bold^ are significantly different than the transcript levels on the other days within that condition (* or ^ $p < 0.05$). Transcripts included c-fos; catalase, Cat; glial-derived neurotrophic factor, Gdnf; glial fibrillary acidic protein, Gfap; interleukin 1β, Il1β; interleukin 6, Il6; superoxide dismutase, Sod2; tumor necrosis factor, Tnfα; and, fibroblast intermediate filament, vim.

Table 5.

Fold changes in transcript expression in the hypothalamus of animals exposed to air or 3D printer emissions after 1, 4, 8, 15, or 30 days of exposure. Exposure to 3DP emissions had very minor effects on the hypothalamus; after 15d if exposure vimentin (Vim) was increased in 3DP emission exposed animals. Transcripts included acetylcholine esterase; Ache; c-fos; calcitonin gene-related peptide (Cgrp); cyclic AMP response element binding protein, Creb; gonadotropin-releasing hormone, GnRH; period 1, Per1; superoxide dismutase 2, Sod2; and, fibroblast intermediate filament, vim.

	Hypothalamus				
transcripts	**1 day**	**4 days**	**8 days**	**15 days**	**30 days**
Ache air	1.02 (0.07)	2.08 (0.64)	1.04 (0.15)	1.22 (0.23)	1.13 (0.25)
3-D emissions	0.84 (0.11)	1.96 (0.50)	0.85 (0.19)	1.36 (0.32)	1.65 (0.23)
c-Fos air	1.31 (0.44)	1.10 (0.36)	1.35 (0.58)	1.12 (0.23)	1.26 (0.35)
3-D emissions	1.88 (0.77)	3.45 (0.62)	2.15 (1.01)	1.83 (0.82)	0.79(0.13)
Cgrp air	1.05 (0.17)	1.89 (1.16)	0.92 (0.16)	1.78 (0.96)	1.08 (0.19)
3-D emissions	1.52 (0.17)	2.04 (1.04)	1.93 (0.88)	1.48 (0.78)	1.44 (0.53)
Creb air	1.05 (0.17)	1.04 (0.12)	0.96 (0.11)	0.94 (0.13)	1.02 (0.09)
3-D emissions	1.11 (0.13)	2.11 (0.52)	0.99 (0.14)	0.90 (0.12)	1.07 (0.09)
Gnrh air	1.18(0.61)	1.30(0.48)	0.98(0.51)	0.53(0.20)	1.54(0.59)
3-D emissions	1.37(0.59)	0.95(0.22)	0.90(0.36)	0.35(0.08)	1.48(0.28)
Per 1 air	1.20 (0.30)	1.81 (1.05)	2.45 (0.99)	1.18 (0.26)	1.22 (0.34)
3-D emissions	1.47 (0.57)	1.06 (0.17)	1.18 (0.26)	1.09 (0.22)	1.28 (0.29)
Sod2 air	1.06 (0.13)	1.45 (0.38)	1.05 (0.15)	1.07 (0.17)	1.09 (0.21)
3-D emissions	0.90 (0.11)	0.48(0.18)	0.97 (0.18)	1.04 (0.15)	1.94 (0.19)
Vim air	1.20(0.33)	1.40(0.53)	1.68(0.76)	**1.68(0.84)**	1.43(0.54)
3-D emissions	1.45(0.52)	0.48(0.18)	0.80(0.35)	**4.55(1.44)***	2.81(1.52)